Open access • Journal Article • DOI:10.1063/1.3026741

Performance improvement of inverted polymer solar cells with different top electrodes by introducing a MoO3 buffer layer — Source link

Chen Tao, Shengping Ruan, Xindong Zhang, Guohua Xie ...+5 more authors

Published on: 13 Nov 2008 - Applied Physics Letters (American Institute of Physics)

Topics: Polymer solar cell, Molybdenum trioxide, Anode, Active layer and Electrode

Performance improvement of inverted polymer solar cells with different top electrodes by introducing a MoO_3 buffer layer

Chen Tao, Shengping Ruan, Xindong Zhang, Guohua Xie, Liang Shen, Xiangzi Kong, Wei Dong, Caixia Liu, and Weiyou Chen[a)]
State Key Laboratory on Integrated Optoelectronics, College of Electronic Science and Engineering, Jilin University, 2699 Qianjin Street, Changchun 130012, People's Republic of China

(Received 7 October 2008; accepted 24 October 2008; published online 13 November 2008)

Molybdenum trioxide (MoO_3) was inserted between the active layer and top electrode in inverted polymer solar cells (PSCs) with nanocrystalline titanium dioxide as an electron selective layer. The performances of structurally identical PSCs with different top electrodes (Au, Ag, and Al) were investigated and compared. The interface between MoO_3 and different metals was studied by x-ray photoelectron spectroscopy. The results showed that the performances of devices with different metals are greatly improved due to the incorporation of MoO_3 and the open-circuit voltage of devices is relatively insensitive to the choice of the anode metal when MoO_3 is introduced. © *2008 American Institute of Physics*. [DOI: 10.1063/1.3026741]

Polymer solar cells (PSCs) based on a blend of conjugated polymers and fullerenes have attracted much attention because of their light weight, low cost, and promising application in the future.[1–4] The performance of PSCs improves remarkably with the introduction of "bulk heterojunction" consisting of an interpenetrating network of electron donor and acceptor materials.[5,6] The power conversion efficiency (PCE) of PSCs based on a blend of regioregular poly(3-hexylthiophene) (RR-P3HT) and highly soluble fullerene derivative 6,6-phenyl C_{61} butyric acid methyl ester (PCBM) has reached up to 5%.[7–9] In these reported devices, poly(3,4-ethylenedioxythiophene):poly (styrenesulfonate) (PEDOT:PSS) is typically spin cast on indium tin oxide (ITO) surfaces to prevent electron leakage and to aid in hole extraction. However, recent research has shown that PEDOT:PSS degraded the performance of device due to its corrosion to ITO.[10,11] In order to solve this problem, one feasible approach is to reverse the device structure by using a less air sensitive and high work function metal as the back hole-collecting electrode. This structure can avoid the use of PEDOT:PSS.

In inverted PSCs, vanadium oxide was usually introduced between the active layer and top electrode as buffer layer.[1,12–14] However, to date the effect of molybdenum trioxide (MoO_3) on the performance of inverted PSCs with different metal electrodes has seldom been reported. In this letter, MoO_3 is introduced between the active layer and top electrode in inverted PSCs with nanocrystalline titanium dioxide (nc-TiO_2) as an electron selective layer. The architecture of the device is shown schematically in Fig. 1(a). The performances of structurally identical PSCs with different top electrodes (Au, Ag, and Al) are investigated and compared. The interface between MoO_3 and different metals is investigated by x-ray photoelectron spectroscopy (XPS).

TiO_2 thin films were prepared by tetrabutyl titanate [$Ti(OC_4H_9)_4$] through a sol-gel method similar to the recipe found in Ref. 15. The procedure for the preparation of TiO_2-sol involved the dissolution of 10 ml $Ti(OC_4H_9)_4$ in 60 ml ethanol (C_2H_5OH), followed by adding 5 ml acetyl acetone. Then a solution, composed of 30 ml C_2H_5OH, 10 ml de-ionized water, and 2 ml hydrochloric acid (HCl) with density of 0.28 mol/l, was added dropwise under vigorous stirring. The final mixture was stirred at room temperature for 2 h.

The patterned ITO-coated glass substrates were sonicated consecutively with acetone, isopropyl alcohol, and deionized water for 10 min. Subsequently TiO_2-sol was spin cast on ITO-coated glass substrates at 3000 rpm. Then the samples were annealed at 450 °C for 2 h in a muffle furnace. For the active layer, the chlorobenzene solution composed of RR-P3HT (10 mg/ml) and PCBM (8 mg/ml) was then spin cast at 700 rpm on top of the nc-TiO_2 layer in air at room temperature. Then the samples were baked in low vacuum (vacuum oven) at ~150 °C for 10 min. Finally the devices were completed with thermal evaporation of MoO_3 and 60 nm top electrode (Au, Ag, and Al). The active area of the device was about 0.064 cm^2.

Current density–voltage (J-V) characteristics of the devices were measured using a computer-controlled Keithley 2601 source meter in air without any device encapsulation. The light source is a 500 W Xe lamp (CHF-XM-500W, Beijing Changtuo). The light intensity was calibrated with a Si photodetector (FZ-A, Photoelectric Instrument Factory of

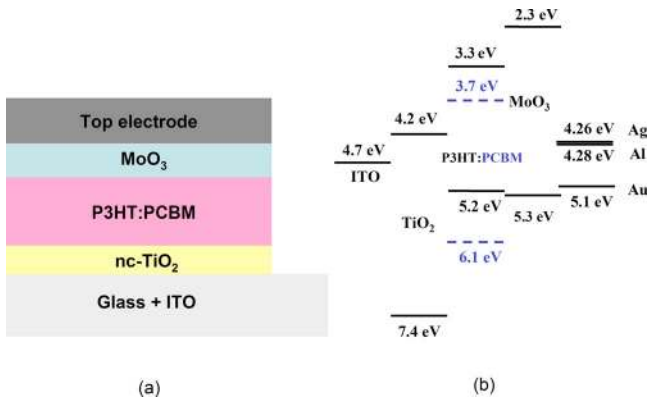

FIG. 1. (Color online) (a) The device structure of the inverted PSCs. (b) Scheme of the energy levels of the materials involved in the inverted PSCs.

[a)]Author to whom correspondence should be addressed. Electronic addresses: chwy@email.jlu.edu.cn and taochen-1984@163.com.

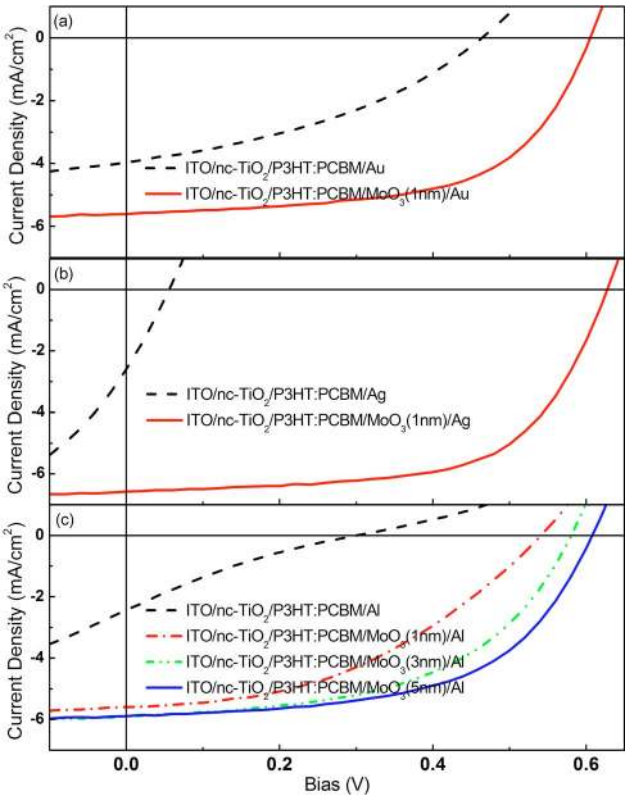

FIG. 2. (Color online) The *J-V* characteristics of devices with different metal electrodes under 100 mW/cm^2 white light illumination: (a) Au, (b) Ag, and (c) Al.

Beijing Normal University). Al $K\alpha$ radiation source ($h\nu$ =1486.6 eV) was used for the XPS analysis, which was carried out in ultrahigh vacuum environment.

Figure 2(a) shows the *J-V* curves of two types of devices, ITO/nc-TiO_2/RR-P3HT:PCBM/Au, and ITO/nc-TiO_2/RR-P3HT:PCBM/MoO_3(1 nm)/Au under 100 mW/cm^2 white light illumination in ambient air. The detailed results are given in Table I. The experiment was carried out with biasing the Au electrode positive. In the absence of the MoO_3 layer, the device exhibits an open-circuit voltage (V_{oc}) of 0.463 V, a short-circuit current density (J_{sc}) of 3.90 mA/cm^2, and a calculated fill factor (FF) of 0.382. The overall PCE ($\eta = I_{sc}V_{oc}FF/P_{in}$, where P_{in} is the incident light intensity) for this cell is therefore only 0.69%. Inclusion of a 1 nm MoO_3 layer between the active layer and Au, the device gives rise to a significant increase in J_{sc} to 5.61 mA/cm^2 and V_{oc} to 0.608 V. Consequently, the PCE improves significantly, rising from 0.69% to 2%.

TABLE I. Short-circuit current density (J_{sc}), open-circuit voltage (V_{oc}), FF, and PCE of inverted PSCs with different anodes.

Anode	J_{sc} (mA/cm^2)	V_{oc} (V)	FF (%)	PCE (%)
Au	3.90	0.463	38.2	0.69
1 nm MoO_3/Au	5.61	0.608	58.6	2.00
Ag	3.11	0.085	26.5	0.07
1 nm MoO_3/Ag	6.57	0.628	62.3	2.57
Al	2.44	0.300	19.1	0.14
1 nm MoO_3/Al	5.60	0.541	42.9	1.30
3 nm MoO_3/Al	5.90	0.581	51.9	1.78
5 nm MoO_3/Al	5.89	0.608	56.4	2.02

Considering the device without MoO_3, both RR-P3HT and PCBM are in direct contact with Au. It is possible for PCBM to transfer electrons to the Au electrode, thereby compromising device efficiency. However, incorporating a MoO_3 layer introduces two additional interfaces (RR-P3HT:PCBM/MoO_3 and MoO_3/Au). The highest occupied molecular orbital (HOMO) level of MoO_3 is −5.3 eV [Fig. 1(b)], which is very close to the HOMO level of RR-P3HT (−5.2 eV). The energy level match reveals that MoO_3 can extract holes from the active layer. The lowest unoccupied molecular orbital level of MoO_3 is −2.3 eV, which is higher than that of PCBM (−3.7 eV). Inserting a MoO_3 layer will prevent electrons from transferring from PCBM to Au. Thus, the MoO_3 interlayer effectively prevents the recombination of the charge carriers at the organic/Au interface. The slope of the *J-V* curve of the device with MoO_3 near 0 V under illumination [Fig. 2(a)] is lower than that of the device without MoO_3, leading to an increase in FF. The FF for the device with MoO_3 is FF=0.586 compared to a value of FF =0.382 for the device without MoO_3.

Similar to devices with Au top electrode, the MoO_3 interlayer is also critical to those with Ag or Al top electrode. By incorporating a MoO_3 buffer layer, the PCE increases from 0.07% to 2.57% for Ag devices [see Fig. 2(b) and Table I] and from 0.14% to 2.02% for Al devices [see Fig. 2(c) and Table I]. At the same time, both J_{sc} and V_{oc} have a significant improvement. All devices with different top electrodes exhibit a PCE of ~2%.[16] The PCE of Ag devices is 0.57% larger than that of Au devices. The possible explanation for this phenomenon is that a small fraction incident light is absorbed by the thermally evaporated Au electrode in Au devices. At the same time, Ag has a higher reflectivity in the visible region compared with Au.[17] The enhanced reflectivity of Ag makes the photocurrent of the devices slightly higher and hence to have a higher PCE. Owing to the oxidization of Al by O_2 in air and the resultant increase of series resistance, Al devices exhibit a lower PCE than Ag devices although Al and Ag have comparable reflectivity in the visible region.

It is observable that for the simple devices, ITO/nc-TiO_2/RR-P3HT:PCBM/top electrode, V_{oc} appears to have considerable differences. V_{oc} are 0.463, 0.085, and 0.3 V, respectively, for the simple devices with Au, Ag, and Al as top electrodes, which do not run parallel to the difference of the work function of these metals [Au (−5.0 eV), Ag (−4.26 eV), and Al (−4.28 eV) (Ref. 18)]. Meanwhile, the low V_{oc} results in poor performance in the simple devices. However, by introducing a thin MoO_3 layer, devices with different metal electrodes exhibit a V_{oc} of ~0.61 V with a variation of 20 mV, leading to a significant improvement in device performance. This suggests that V_{oc} of device with MoO_3 is independent of the work function of the top electrodes.

It is known that V_{oc} is the voltage where the applied bias equals the built-in potential in an ideal diode. In Au or Ag devices, 1 nm MoO_3 is thick enough to increase the built-in potential. However, V_{oc} does not reach to ~0.61 V in Al devices until the thickness of MoO_3 is 5 nm. Prior to metal deposition, the fabrication conditions for devices are held constant. The sole differential is the interface between MoO_3 and electrode metals. We deduce that the chemical reaction between MoO_3 and Al occurs during thermal evaporation of Al. However, contact of MoO_3 with Au or Ag is physical.

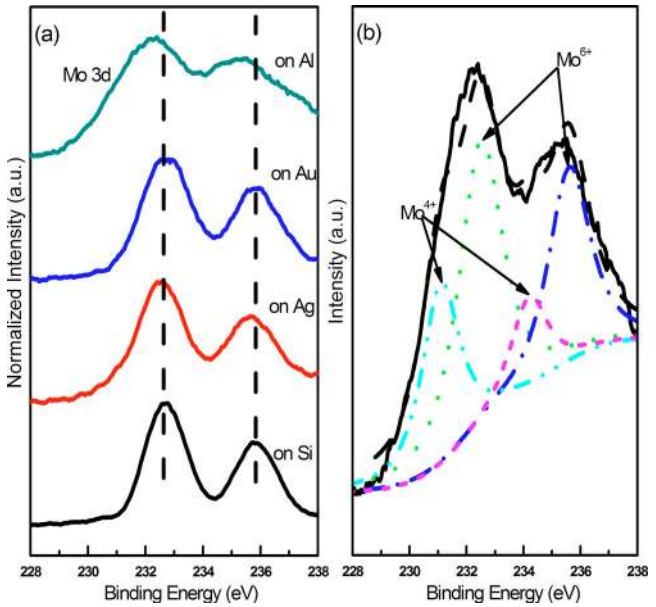

FIG. 3. (Color online) (a) XPSs of Mo 3*d* doublet for thermally evaporated MoO_3 on Si, Au, Ag, and Al substrates. (b) XPS peak fitting of Mo 3*d* doublet for thermally evaporated MoO_3 on Al substrate.

In order to investigate the interface between MoO_3 and different metals, XPS is introduced. Figure 3(a) shows Mo 3*d* spectra from XPS study of 5 nm MoO_3 film thermally evaporated on different substrates. For MoO_3 on Si, Au, and Ag substrates, the Mo 3*d* spectra show the presence of two well resolved spectral lines at 232.60–232.75 and 235.65–235.75 eV, which are assigned to the Mo $3d_{5/2}$ and $3d_{3/2}$ spin-orbit components, respectively. However, compared with MoO_3 on Si, Au, and Ag substrates, both Mo $3d_{5/2}$ and $3d_{3/2}$ peaks for MoO_3 on Al substrate shift obviously toward a lower binding energy and the full width at half maximum (FWHM) broadens.

Figure 3(b) shows XPS peak fitting of Mo 3*d* spectra for MoO_3 on Al substrate. In the fitting of complex signal shapes, the main constrain is that the binding energy difference ΔE_B of Mo $3d_{3/2}$ and $3d_{5/2}$ is 3.1 ± 0.1 eV, which ensures that the results have the corresponding physical senses.[19] The peak fitting results indicate that some of the MoO_3 present on the Al surface is transformed to MoO_2 as indicated by the additional spectral lines positioned at 231.15 and 234.25 eV. These double peaks represent Mo^{4+} in MoO_2.[20] Thus we infer that partial MoO_3 can be reduced to MoO_2 by Al during thermal evaporation of Al. This is consistent with the thermal analysis of Al–MoO_3 nanocomposites by Swati *et al.*[21] MoO_2 is a conductor, which would not affect the charge transport in Al devices. As a result, it needs a thicker MoO_3 layer in Al devices than in Au or Ag devices due to the chemical reaction between MoO_3 and Al.

In summary, we have introduced an efficient structure of inverted PSCs with nc-TiO_2 as an electron selective layer by inserting a MoO_3 layer between the active layer and top electrode. The performances of structurally identical PSCs with different top electrodes (Ag, Au, and Al) are investigated and compared. All devices exhibit a PCE of ~2% under 100 mW/cm^2 white light illumination. The MoO_3 interlayer effectively prevents the recombination of charge carriers at the organic/top electrode interface, leading to the improvement of J_{sc}, V_{oc}, and FF. Devices with different top electrodes exhibit a V_{oc} of ~0.61 V. It is suggested that V_{oc} is irrespective of the work function of top electrode. XPS research indicates that the contact between MoO_3 and Al is different from that between MoO_3 and Au (or Ag). Due to chemical reaction between MoO_3 and Al, the thickness of the MoO_3 layer is thicker in Al devices than in Au or Ag devices when V_{oc} reaches up to ~0.61 V.

The authors are grateful to Major Project of Science and Technology Development Plan of Jilin Provincial Science and Technology Department (Grant Nos. 20070402 and 20080330) and the National Natural Science Foundation of China (Grant No. 60877041) for the support of the work.

[1] G. Li, C.-W. Chu, V. Shrotriya, J. Huang, and Y. Yang, Appl. Phys. Lett. **88**, 253503 (2006).
[2] J. Y. Kim, S. H. Kim, H.-H. Lee, K. Lee, W. Ma, X. Gong, and A. J. Heeger, Adv. Mater. (Weinheim, Ger.) **18**, 572 (2006).
[3] T. Offermans, S. C. J. Meskers, and R. A. J. Janssen, Org. Electron. **8**, 325 (2007).
[4] G. Dennler, A. J. Mozer, G. Juška, A. Pivrikas, R. Österbacka, A. Fuchsbauer, and N. S. Sariciftci, Org. Electron. **7**, 229 (2006).
[5] G. Yu, J. Gao, J. C. Hummelen, F. Wudl, and A. J. Heeger, Science **270**, 1789 (1995).
[6] N. S. Sariciftci, L. Smilowitz, A. J. Heeger, and F. Wudl, Science **258**, 1474 (1992).
[7] W. Ma, C. Yang, X. Gong, K. Lee, and A. J. Heeger, Adv. Funct. Mater. **15**, 1617 (2005).
[8] M. Reyes-Reyes, K. Kim, and D. L. Carroll, Appl. Phys. Lett. **87**, 083506 (2005).
[9] G. Li, V. Shrotriya, J. Huang, Y. Yao, T. Moriarty, K. Emery, and Y. Yang, Nature Mater. **4**, 864 (2005).
[10] Y.-H. Kim, S.-H. Lee, J. Noh, and S.-H. Han, Thin Solid Films **510**, 305 (2006).
[11] M. P. de Jong, L. J. van Ijzendoorn, and M. J. A. de Voigt, Appl. Phys. Lett. **77**, 2255 (2000).
[12] H. H. Liao, L. M. Chen, Z. Xu, G. Li, and Y. Yang, Appl. Phys. Lett. **92**, 173303 (2008).
[13] K. Takanezawa, K. Tajima, and K. Hashimoto, Appl. Phys. Lett. **93**, 063308 (2008).
[14] B. Y. Yu, A. Tsai, S. P. Tsai, K. T. Wong, Y. Yang, C. W. Chu, and J. J. Shyue, Nanotechnology **19**, 255202 (2008).
[15] H. L. Xue, X. Z. Kong, Z. R. Liu, C. X. Liu, J. R. Zhou, and W. Y. Chen, Appl. Phys. Lett. **90**, 201118 (2007).
[16] Note that the power conversion efficiencies of our devices are lower than the ones reported in the literature because of all devices being fabricated and tested in ambient atmosphere. However, the blended active layer was baked in low vacuum (vacuum oven).
[17] S. Chen, Y. Zhao, G. Cheng, J. Li, C. Liu, Z. Zhao, Z. Jie, and S. Liu, Appl. Phys. Lett. **88**, 153517 (2006).
[18] C. J. Brabec, A. Cravino, D. Meissner, N. S. Sariciftci, T. Fromherz, M. T. Rispens, L. Sanchez, and J. C. Hummelen, Adv. Funct. Mater. **11**, 374 (2001).
[19] W. Grünert, A. Y. Stakheev, R. Feldhaus, K. Anders, E. S. Shpiro, and K. M. Minachev, J. Phys. Chem. **95**, 1323 (1991).
[20] B. Brox and I. Olefjord, Surf. Interface Anal. **13**, 3 (1988).
[21] S. M. Umbrajkar, M. Schoenitz, E. L. Dreizin, and E. Propellants, Propellants, Explos., Pyrotech. **31**, 382 (2006).